

Depletion Effects and Loop Formation in Self-Avoiding Polymers

N. M. Toan,¹ D. Marenduzzo,² P. R. Cook,³ and C. Micheletti¹

¹International School for Advanced Studies (SISSA) and CNR-INFM, Via Beirut 2-4, 34014 Trieste, Italy

²SUPA, School of Physics, University of Edinburgh, Mayfield Road, Edinburgh, EH9 3JZ, United Kingdom

³Sir William Dunn School of Pathology, University of Oxford, South Parks Road, Oxford, OX1 3RE, United Kingdom

(Received 9 June 2006; published 26 October 2006)

Langevin dynamics is employed to study the looping kinetics of self-avoiding polymers both in ideal and crowded solutions. A rich kinetics results from the competition of two crowding-induced effects: the depletion attraction and the enhanced viscous friction. For short chains, the enhanced friction slows down looping, while for longer chains, the depletion attraction renders it more frequent and persistent. We discuss the possible relevance of the findings for chromatin looping in living cells.

DOI: 10.1103/PhysRevLett.97.178302

PACS numbers: 82.35.Lr, 82.35.Pq, 82.70.Dd

The kinetics and thermodynamics of the folding of a flexible polymeric chain into a loop are central issues in polymer physics [1–4]. Renewed interest in this classic problem has been fueled by the introduction of novel manipulation techniques [5] that provide unprecedented insight into the mechanics and flexibility of various biopolymers. In particular, it has been shown that, in the cell nucleus, DNA regions separated by several μm 's on the genetic map can nevertheless be in molecular contact [5]. Is such looping generated by *active* mechanisms (e.g., molecular motors) or merely by *passive* thermodynamic mechanisms (e.g., diffusion)? Some light can be shed on these issues by comparing experimental observations with the statistics and dynamics of looping predicted by general polymer models. The systematic application of this strategy has so far been hindered by the dependence of cyclization dynamics on many time scales even for the simplest phantom polymer models [6].

Here, we go beyond the treatment of phantom chains and focus on the impact of steric effects. We not only consider the polymer self-avoidance [1,7] but also incorporate excluded volume interactions of the chain with a surrounding crowded environment, treated as a collection of small monodisperse globular particles (microspheres) which induce an entropic attraction on larger objects in solution [8]. To date, the investigation of this intriguing *depletion effect* has been mainly studied in polydispersed colloidal solutions [8,9]. Understanding how crowding affects the behavior of a single self-avoiding polymer thus represents a novel and important topic in macromolecular physics. It also has immediate implications in cell and systems biology, as cells are so crowded with globular proteins and RNAs [10–13]. We show that crowding affects the occurrence and persistence of loops in self-avoiding polymers in diverse ways, according to the length of the polymer chain and the size of the constitutive monomers. Besides uncovering new physics, our results may be relevant to the understanding of chromatin looping *in vivo*. Specifically, we will discuss whether and to what extent the depletion attraction may explain existing observations in cell biology

that active polymerases, attached to chromatin, cluster into supramolecular “factories” of up to μm size during transcription and replication [13].

A traditional string-and-beads model will be used to describe polymer chains. We consider two simple cases: a plain self-avoiding string of N equally-sized spherical beads of radii $R_{i=1,\dots,N} = 12.5$ nm, and one with larger beads at the ends. This sphere size was chosen to relate our polymer to an eukaryotic chromatin fiber, whose effective diameter and persistence length are both ~ 25 nm [14]. The case of larger end beads is instead motivated by the study of chromatin loops with an attached genome-grabbing machinery (a large transcription or a replication complex which locally increases the effective fiber diameter [13]). The potential energy, when the centers of beads i and j are at a distance $d_{i,j}$, is

$$V_c = \epsilon_1 \sum_{i < j} e^{-a(d_{i,j} - d_{ij}^0)} - \epsilon_2 \sum_i \ln \left[1 - \left(\frac{d_{i,i+1}}{1.5d_{i,i+1}^0} \right)^2 \right] \quad (1)$$

where ϵ_1 and ϵ_2 are, respectively, 0.24 and 70 units of thermal energy, $\kappa_B T$, $a = 4$ nm⁻¹, and $d_{i,j}^0 = R_i + R_j$ is the contact distance of beads i . The first term in Eqn. (1) enforces the hard-core repulsion for contacting pairs, while the second provides an attraction between consecutive beads on the chain. Interplay between the two terms produces a self-avoiding finitely extensible nonlinear elastic (FENE) chain [15] where, at temperature $T = 300$ K, the distance between consecutive beads fluctuates by about 0.5 nm around 25 nm. The microspheres have radius $r = 2.5$ nm and occupy a fraction $\phi = 0.15$ of the total available volume. These values conservatively reflect the crowding of the cellular environment mostly due to RNA and proteins [13]. Because the value of ϕ considered here is moderate [see Fig. 1(a)], we can resort to the approximate Asakura-Oosawa (AO) treatment [8], which *does not* require simulating explicitly the dynamics of microspheres. More precisely, in addition to the term of Eqn. (1), the polymer is subject to the following effective interaction potential:

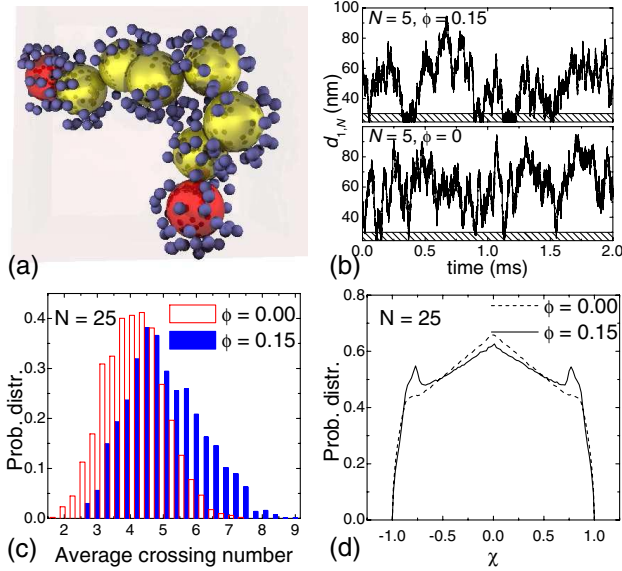


FIG. 1 (color online). (a) Sketch of a chain of $N = 8$ beads (end spheres highlighted) of radius $R = 12.5$ nm. Microspheres ($r = 2.5$ nm and $\phi = 0.15$) within 7.5 nm of the chain surface are shown. (b) Time evolution of the end-to-end distance, $d_{1,N}$, in chains of $N = 5$ beads, subject to the effective depletion potential accounting for the presence ($\phi = 0.15$) and absence ($\phi = 0$) of the microspheres. Looping occurs when $d_{1,N} < 2(R + r) = 30$ nm (shaded area). Probability distribution of (c) average crossing number and (d) chirality for $\phi = 0$ and $\phi = 0.15$.

$$V_{AO} = -\frac{\phi k_B T}{16r^3} \sum_{i < j} \left(2\tilde{d}_{ij} + 3d_{ij} - \frac{3\Delta_{ij}^2}{d_{ij}} \right) \tilde{d}_{ij}^2 \Theta[\tilde{d}_{ij}] \quad (2)$$

where $\tilde{d}_{ij} = 2r + d_{ij}^0 - d_{ij}$, $\Delta_{ij} = |R_i - R_j|$, and the step function Θ ensures that the AO depletion interaction vanishes at distances $> d^0 + 2r$ [8]. As r is sufficiently smaller than the radii of the chain beads, it is legitimate to disregard in (2) three- and many-body interactions. The evolution of the system, carried out for various N , sizes of end spheres, and values of ϕ , was described by overdamped Langevin dynamics

$$\gamma_i \dot{x}_i^\alpha = -\partial(V_c + V_{AO})/\partial x_i^\alpha + \xi_i^\alpha(t), \quad (3)$$

where α runs over the Cartesian components, \vec{x}_i is the position of the i th bead, and the stochastic white noise term obeys the fluctuation-dissipation condition: $\langle \xi \rangle = 0$, $\langle \xi_i^\alpha(t) \xi_j^\beta(t') \rangle = 2\delta_{\alpha,\beta} \delta_{i,j} \delta(t, t') k_B T \gamma_i$. The friction term γ_i was obtained from the Stokes-Einstein [1] relationship: $\gamma_i = 6\pi\eta(1 + 2.5\phi)R_i$ where $\eta = 5$ cP [13]. The Langevin equation was integrated numerically by means of a predictor-corrector scheme [16] and a time step of 15 ps. The viability of Eqn. (3) was ascertained by a preliminary successful comparison of various dynamic and equilibrium properties with those produced by underdamped dynamics (with masses deduced from typical densities of biopolymers, $\rho = 1.35$ g/cm³ [17]).

The dynamical evolution was followed starting from randomized non self-intersecting configurations of chains with $3 \leq N \leq 30$ beads. When investigating how looping dynamics is affected by the size of the contacting spheres, we set $N = 10$ and varied the radius of the end spheres, $R_1 = R_N$, within 12.5 and 43.75 nm. The formation of loops was detected by monitoring the end-to-end distance, $d_{1,N}$, and comparing it to the range of the depletion attraction, $d_{1,N} < (d_{1,N}^0 + 2r)$. To have a well-defined comparison term, the same criterion for loop formation was adopted in the absence of crowding effects or agents (i.e., $\phi = 0$). Typical evolutions of the end-to-end distance are illustrated in Fig. 1(b). The trajectories were analyzed to highlight how depletion interactions affect the looping kinetics and the chain's equilibrium structural properties. For the latter issue several geometrical descriptors were considered: the radius of gyration, virial coefficients, and the distribution of local chiralities $\chi_i = \vec{u}_{i+2,i+3} \cdot (\vec{u}_{i,i+1} \wedge \vec{u}_{i+1,i+2})$, $\vec{u}_{i,i+1}$ being the normalized bond vector joining residues i and $i + 1$. For looped configurations, we also calculated the writhe and crossing number, averaged over hundreds of randomly oriented two-dimensional projections [18]. Concerning the looping dynamics, we instead characterize the evolution of the system in terms of the mean-first looping time (MFLT) and the mean-first unlooping time (MFUT), which we establish through the following novel procedure apt for numerical implementation. For very long, and hence thermalized, trajectories the MFLT is obtainable by picking at random unlooped conformations and measuring the time to the first looping event. Configurations in a specific “unlooped time interval” of duration τ_u will be picked with weight equal to τ_u , and their average first looping time will be $\tau_u/2$. The MFLT can thus be expressed in terms of the average duration of unlooping intervals and its second moment: $\text{MFLT} = \frac{1}{2} \times \frac{\langle \tau_u^2 \rangle}{\langle \tau_u \rangle}$. An analogous formula holds for the MFUT. The average values of MFUT and MFLT (we have verified that the first two moments of looping and unlooping intervals are finite) and their uncertainties were calculated over 10 independent trajectories having maximum duration ranging from 0.1 s for $N = 3$ to 10 s for $N = 30$.

We first discuss the structural differences of the generated configurations. The short-range depletion attraction produces a reduction of the effective size of the polymer. For the largest N considered, where most conformations are unlooped, the radius of gyration decreases by 10% when ϕ goes from 0 to 0.15. The depletion attraction also impacts on the chain structural organization. Indeed, the geometrical complexity of looped chains is enhanced by crowding and the average crossing number increases with ϕ [Fig. 1(c)]. This is akin to what occurs in random rings upon compactification [18]. At variance with this case, the development of a striking trimodal character of the chirality distribution, indicates the emergence of a peculiar structural organization [see Fig. 1(d)]. Though the chiral biases are local, and hence do not lead to long-

range structural order, they provide qualitative support to the recent suggestion of Snir and Kamien that depletion effects may be sufficient to drive the formation of optimal helices in thick biopolymers [11,19].

We next turn to the analysis of the looping kinetics and discuss the behavior of the MFUT. In the presence of microspheres, the two contacting ends are subject to the depletion attraction, and it may be anticipated that the MFUT is larger than for $\phi = 0$. This expectation, qualitatively perceivable from Fig. 1(b), is confirmed and quantified in Fig. 2(a) which portrays a parallel trend of unlooping time as a function of N for $\phi = 0$ and $\phi = 0.15$. Moderate crowding is enough to increase the time the ends spend together (forming a loop) by a factor of 3.

The behavior of the MFLT [Fig. 2(c) and 2(d)] is more intriguing and harder to anticipate, owing to two opposing tendencies. On one hand, as we saw earlier, the depletion attraction reduces the effective polymer size and hence favors looping. On the other, crowding augments the effective viscosity of the medium, thereby slowing the diffusive encounter of terminal beads. More precisely, the Stokes-Einstein formula gives a 38% increase of friction coefficient when $\phi = 0.15$ compared to $\phi = 0$. The resulting balance between the two opposing effects can be established by considering the asymptotic expression for relaxation times in Rouse chains with excluded volume. The slowest relaxation time in such chains (assimilated to the MFLT [6,7]) increases as $\gamma b^2 N^{2\nu+1}$, where $\nu \approx 0.6$ is the scaling exponent for self-avoiding polymers and b is the effective size of the chain monomers estimated by calculating the second virial coefficient accounting for the depletion attraction of Eqn. (2) [1]. Indeed, the

data collected within the explored range of N appear well compatible with this asymptotic relationship [see Fig. 2(c)]. The Rouse scaling formula can hence be used to quantify how the crowding-induced changes in γ and b ultimately affect the MFLT for large N . For the specific case considered here, $\phi = 0.15$, one finds that the MFLT is *decreased* by about 17% compared to the $\phi = 0$ case. This crude asymptotic estimate is in fair agreement with the simulation results for $N = 15-30$, which indicates that, when $\phi = 0.15$, crowding decreases the MFLT by 10% or more. It is interesting to consider, within the previous approximate analysis, how the MFLT depends on ϕ . This information, obtained from the known functional dependence on ϕ of the friction and second virial coefficients, is shown in Fig. 3 which portrays an intriguing nonmonotonic dependence: for small crowding $\phi < 0.1$, the diffusive slowing dominates, while larger ϕ facilitate looping via depletion-induced crumpling of the chain.

We finally discuss the dependence of looping on the size of the terminal beads. We considered chains of $N = 10$ beads where $R_1 = R_N$ were varied between 12.5 and 43.75 nm. We found that the increase in end spheres size had minor effect on the MFLT which, for $\phi = 0.15$, changed by less than 10% over the explored range of terminal radii. The near constancy of the MFLT is noteworthy since the change of $R_1 = R_N$ from 12.5 to 43.75 nm implies a two-fold increase of probability that terminal spheres contact internal ones. In contrast, the MFUT is greatly affected by changes in terminal radii. As illustrated in Fig. 2(b) for $\phi = 0.15$, it increases approximately exponentially as a function of R_1 and R_N . This behavior would be expected if the terminal bead exited the depletion well (whose depth increases linearly with $R_1 = R_N$) according to simple Arrhenius kinetics. However, the increase in MFUT also reflects the decreased diffusivity of terminal beads as a result of the linear increase in R of the friction coefficient, γ . This second effect, dominated by the former in the presence of crowding, is readily visible in the curve pertaining to $\phi = 0$ in Fig. 2(b). The dotted line represents a fit to the 6 data points with a linear relationship in $R_1 = R_N$ (with relative χ^2 equal to 1.5), which would be appropriate if the diffusion coefficient of the terminal

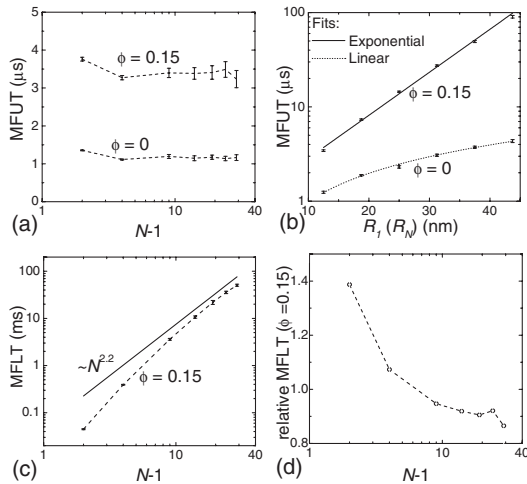


FIG. 2. Mean-first unlooping time as a function of (a) chain length and (b) radius of terminal spheres. The curved lines in (b) correspond to exponential and linear fits of the data. (c) Mean-first looping time as a function of chain length (points and dashed line). The asymptotic law for relaxation time in Rouse chains, $\tau_R \propto N^{2\nu+1}$, is shown for comparison. (d) Ratio between MFLT in the presence ($\phi = 0.15$) and absence ($\phi = 0$) of crowding agents. The typical error is 5%.

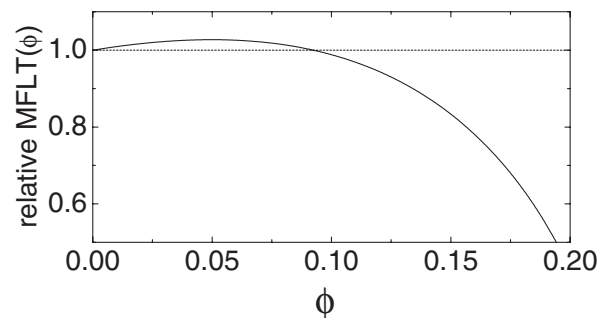


FIG. 3. Theoretical behavior of the ratio between MFLT at finite volume crowding, ϕ , and the MFLT ($\phi = 0$).

spheres were the only factor slowing unlooping. By carrying out simulations for selected values of ϕ , it was found that increasing ϕ enhances the magnitude of these effects. For example, with $\phi = 0.3$, which may also be appropriate for crowding in nucleoplasm [13], the MFLT is ~ 3 times smaller and the MFUT (with $R_1 = R_N = 25$ nm) ~ 9 times longer than with $\phi = 0.15$.

We now discuss the possible biological implications of our results. As mentioned previously, a large number of active DNA (and RNA) polymerases can attach to specific segments of a chromatin fiber, thus increasing its local thickness. Experimental observations have shown that these scattered groups of polymerases eventually cluster into replication (or transcription) factories, thus looping the intervening genome. In the case of replication factories in eukaryotes, these structures contain ~ 10 or more polymerases and range in size from ~ 100 nm up to $\sim \mu\text{m}$ [13]. Is there a simple physical mechanism leading to their establishment? Our study suggests that the formation and persistence of these loops can be aided by cellular crowding. First, using a conservative estimate of $\phi = 0.15$, we find that the depletion self-interaction of the fiber thermodynamically facilitates looping (see, e.g., Fig. 1). For example, analysis of end-to-end distances in equilibrium shows that bridging the two ends of a 750-nm fiber, which would contain 75 kilobases of DNA [14], costs more than $8 k_B T$ in the absence of crowding agents, but less than $7 k_B T$ in their presence. We find crowding diminishes the looping cost by $1\text{--}2 k_B T$ for all lengths simulated. All, or most, of this looping cost may be overcome by the extra depletion attraction between the thicker ends of the loop, to which the replication machinery is attached, consistently with recent theoretical predictions [13]. Second, the results of Fig. 2(d) demonstrate that crowding can also aid looping *dynamically* by facilitating the diffusive encounter of the ends. This intriguing result is supported by theoretical arguments summarized in Fig. 3, which suggest the effect is robust. Furthermore, crowding stabilizes loops *once the two ends have met*. The fact that the MFUT has an approximately exponential dependence on the height of the depletion well [Fig. 2(b)] underscores the role that crowding has for the formation of replication or transcription factories. Via Eqn. (2), the unlooping time of, e.g., two transcription complexes of radius $R \approx 40$ nm with $\phi \approx 0.3$ is estimated to easily exceed 0.1 s—a macroscopic time scale comparable to the experimentally measured persistence time of factories. In living cells the lifetime of such aggregates is probably longer because, besides other physical-chemical factors, many complexes may come together (rather than the two considered here), and interactions of one large bead with two or more others cooperatively increases the stabilization due to the depletion attraction [13].

In conclusion, we have considered various kinetic and thermodynamic aspects of polymer looping in a crowded medium. The process of loop formation is controlled by

two opposing effects. On one hand, looping is entropically aided in crowded media by the depletion effect. On the other, the enhanced friction of the medium hinders the diffusive encounter of the chain ends. The balance of the two effects is found to depend both on the length of the polymer chain and on the size of the contacting ends. Specific model parameters have been used to show quantitatively that crowding-enhanced looping formation or persistence may be actually exploited in living cells to promote the contact of actively replicated/transcribed chromatin regions as observed in recent experiments [13]. The approach outlined here demonstrates the viability of computational and analytical approaches to investigate the novel and stimulating problem of crowding effects on a single polymer. It would be interesting to confront theory and experiments on looping and unlooping times obtained from single molecules experiments with and without crowding agents.

-
- [1] M. Doi and S.F. Edwards, *The Theory of Polymer Dynamics* (Clarendon Press, Oxford, 1986).
 - [2] G. Wilemski and M. Fixman, *J. Chem. Phys.* **60**, 878 (1974); A. Szabo, K. Schulten, and Z. Schulten, *J. Chem. Phys.* **72**, 4350 (1980); M. Muthukumar, *Proc. Natl. Acad. Sci. U.S.A.* **96**, 11 690 (1999).
 - [3] R. Metzler *et al.*, *Phys. Rev. Lett.* **88**, 188101 (2002).
 - [4] E. Carlon, E. Orlandini, and A. L. Stella, *Phys. Rev. Lett.* **88**, 198101 (2002).
 - [5] J. Dekker *et al.*, *Science* **295**, 1306 (2002); L. Chakalova *et al.*, *Nat. Rev. Genet.* **6**, 669 (2005); J. Vilar and L. Saiz, *Curr. Opin. Genet. Dev.* **15**, 136 (2005).
 - [6] S. Jun., J. Bechhoefer, and B.-Y. Ha, *Europhys. Lett.* **64**, 420 (2003); J.Z. Y. Chen, H.-K. Tsao, and Y.-J. Sheng, *Phys. Rev. E* **72**, 031804 (2005).
 - [7] A. Podtelezhnikov and A. Vologodskii, *Macromolecules* **30**, 6668 (1997).
 - [8] D. Asakura and F. Oosawa, *J. Polym. Sci.* **33**, 183 (1958); Y. Mao, M.E. Cates, and H.N.W. Lekkerkerker, *Phys. Rev. Lett.* **75**, 4548 (1995); B. Gotzelmann, R. Evans, and S. Dietrich, *Phys. Rev. E* **57**, 6785 (1998).
 - [9] R. Verma *et al.*, *Phys. Rev. Lett.* **81**, 4004 (1998); J.C. Crocker *et al.*, *Phys. Rev. Lett.* **82**, 4352 (1999).
 - [10] M. S. Cheung, D. Klimov, and D. Thirumalai, *Proc. Natl. Acad. Sci. U.S.A.* **102**, 4753 (2005).
 - [11] Y. Snir and R. D. Kamien, *Science* **307**, 1067 (2005).
 - [12] A. P. Minton, *J. Biol. Chem.* **276**, 10 577 (2001).
 - [13] P. R. Cook, *Science* **284**, 1790 (1999); *Nat. Genet.* **32**, 347 (2002); D. Marenduzzo, C. Micheletti, and P. R. Cook, *Biophys. J.* **90**, 3712 (2006).
 - [14] H. Schiessel, *J. Phys. Condens. Matter* **15**, R699 (2003).
 - [15] K. Kremer and G.S. Grest, *J. Chem. Phys.* **92**, 5057 (1990).
 - [16] M.P. Allen and D.J. Tildesley, *Computer Simulation of Liquids* (Clarendon Press, Oxford, 1991).
 - [17] B. W. Matthews, *J. Mol. Biol.* **33**, 491 (1968).
 - [18] C. Micheletti *et al.*, *J. Chem. Phys.* **124**, 064903 (2006).
 - [19] A. Maritan *et al.*, *Nature (London)* **406**, 287 (2000); J. E. Magee *et al.*, *Phys. Rev. Lett.* **96**, 207802 (2006).